Chapter 2
Conceptual Design

H. Baier, M. Hornung, B. Mohr, D. Paulus, Ö. Petersson, C. Rößler, F. Stroscher and T. Salmon

2.1 Introduction

Highly efficient future aircraft configurations are needed in order to cope with ever-growing air traffic and to sustain and improve passenger comfort and freight requirements. The configurations within the project ACFA 2020 are designed for the growing mid-range and long-haul market segments of 400 passengers and beyond. Airbus considers the biggest market share with 42 % order value from 2010 to 2029 to be taken by mid-size twin aisle aircraft. If long-range large aircraft are included, new order value rises to 60 % [4].

Two aircraft configurations were investigated in AFCA 2020. The superior design was chosen to be further analyzed. Active control was investigated as a means to increase aerodynamic efficiency and to improve ride comfort. Since active control not only directly influences the control surfaces, the conventional aircraft design process had to be adapted at an early stage of development. Tailless aircraft configurations with wing-fuselage blending potentially offer low fuel consumption, mainly achieved by drag reduction, reduced structural weight, and by the significantly lower wetted area ratio [5, 7]. Exterior noise can be minimized by an advanced high-lift system or by shielding of the engines [1]. Airframe development for a blended wing body (BWB) and a wide body configuration with carry-through wing box (CWB), as the basis for further control studies, was conducted within the first year of the project.

This chapter discusses the conceptual aircraft design and selection process of a highly efficient BWB and CWB configuration on a specified design mission. The challenges and development methods are described beginning with the requirements definition. The main body will present the results of the design process with a special

H. Baier (✉) · M. Hornung · B. Mohr · D. Paulus · Ö. Petersson · C. Rößler · F. Stroscher
Technische Universität München, Munich, Germany
e-mail: baier@tum.de

T. Salmon
Airbus Operations S.A.S., Toulouse, France

focus on the multidisciplinary design optimization (MDO) of the fuselage and wing box. Systematically comparing the developed configurations led to the selection of an aircraft that is most suitable for the proposed mission and further development. This chapter is adapted with slight modifications from [10].

2.2 Requirements and Mission Definition

A set of requirements for operational performance, fuel and passenger capacities was established with project partners [8]. The most relevant requirements are given in the following.

2.2.1 Operational Performance

Global requirements begin with the mission definition as shown in Table 2.1. The development focuses on a carrier design for at least 460 passengers (Pax) on a 7,200 nautical mile mission in a two-class layout. Flight altitude is 33,000 ft and higher, with a cruise Mach number of 0.85. The aircraft must be able to fly at its optimum altitude during the entire cruise phase, for which climb and buffet ceilings were defined. For slow approaches, a speed of less than 150 knots is considered to be optimal [1].

2.2.2 Passenger Cabin and Landing Gear Definition

For the BWB, the baseline layout is a two-class arrangement with a total of 470 passengers in a business class (BC)/economy class (YC) class splitting of 56/414. On the other hand, the CWB has a two-class arrangement with 464 passengers in BC/YC splitting of 60/404. For the landing gear, a wheel track of less than 16 m (International Civil Aviation Organization (ICAO) Code F) and a rotation clearance angle of greater than 11° shall be achieved.

Table 2.1 ACFA mission definition

ACFA global requirements	
Approach speed	<150 kt
Range	≥7,200 nm
Cruise Mach number	0.85
Initial cruise altitude	≥33,000 ft
Pax	≥460 in two-class layout

2.2.3 Lifting Surface Requirements

New aircraft wing span is restricted to 80 m under the International Civil Aviation Organization (ICAO) Code F. Winglets for yaw control, in the event that one engine is inoperative, are an option. The leading-edge sweep angle shall be 55° for the BWB center body.

The BWB outer wing and CWB wing sweep and relative thickness need to be designed to optimize the fuel burn of the overall aircraft in an aerodynamic performance/weight trade-off. Hence, the BWB center body's maximum relative thickness should not exceed 17 %. The spanwise load distribution target in the early phase is elliptic as it has been identified as a potential optimum, since a large part of the flying wing structure is not sized by aerodynamic loading but by pressurization.

2.2.4 Fuel Capacity

Fuel capacity is set to be greater than the maximum take-off weight (MTOW) minus operating empty weight (OWE) plus 0.7 times the two-class payload. For 464 passengers and an assumed 105 kg per passenger, the payload sums up to 48,720 kg. This results in the basic fuel capacity formula (2.1):

$$m_{\text{Fuel}} > \text{MTOW} - \text{OWE} - 34{,}104\,\text{kg} \qquad (2.1)$$

2.3 Design Process

This section describes the design methods and processes applied to the CWB and BWB configurations based on the preceding definition of global requirements.

2.3.1 Structural Weight

2.3.1.1 Fuselage Design

The fuselage was sized according to cabin and passenger requirements. For unconventional fuselage shapes, the methods applied for current commercial aircraft with an aft empennage are not applicable. Foregoing parametric studies of cross section with different radii and structural thickness were optimized in close cooperation with the Institute of Lightweight Structures (see Chap. 3). The cabin integration for unconventional aircraft designs revealed the necessity of using finite element (FE) models to obtain mass and center of gravity estimates for the fuselage, since

conventional statistical equations cannot be applied for the unconventional cross
section. Both layouts were optimized for cross-sectional and wetted area. In addi-
tion, the provision of six exits at each side and an easy loading and unloading of the
unit load devices 3 (LD) and pallets is foreseen. A cruise angle of attack of less than
3° at 1.7° can be considered as comfortable.

2.3.1.2 Wing

The Luftfahrttechnisches Handbuch (engl. Aviation Technology Handbook) (LTH),
a German aerospace publication for civil and military aircraft applications [2], was
used for BWB and CWB wing weight calculations and also applied for the slats,
flaps, and ailerons including paint. After the establishment of the FE model, wing
weight calculations were compared with the analytical model and FE results were
used for a more detailed concept development.

2.3.1.3 Conventional Structural Elements

The weights of the structural elements which do not significantly differ from con-
ventional design were computed from the LTH [2]. The results were either directly
calculated or validated with published data. As mentioned above, the fuselage pri-
mary structure was designed with a FE model. Secondary structure elements, such
as cabin and cargo floors, doors, landing gear (main/front), cockpit and cabin win-
dows, horizontal and vertical stabilizers, engines including the controls, subsystems,
oxygen, and deicing systems, were also calculated according to the LTH [2]. Fur-
ther systems in this calculation included communication, electric wiring, furnishing,
water installation, and operator items.

2.3.2 Aerodynamics and Control

2.3.2.1 Subsonic Regime

To ensure the comparability of the CWB to the BWB configuration, the same meth-
ods and approach for both configurations were used. The core is a combination of
empirical equations to calculate the aerodynamic efficiency at trimmed conditions.
With these equations, variable parameters have been optimized to attain maximum
aerodynamic efficiency at different angles of attack and flight altitudes. In addition,
a vortex lattice method with 3D panels was used to develop the profiles and to calcu-
late pressure and lift distributions. The BWB requires specially designed airfoils as
stability has to be achieved through sweep and twist adjustments. The center section
has to accommodate the cabin box which decreases aerodynamic performance in the
transonic speed region. The three-dimensional target lift distribution was achieved

by iterating the local twist and spanwise twist with specially adapted airfoils with a half-span partition into five wing panels. Hence, low lift coefficients are required in the middle section and higher lift coefficients at the outer parts of the wing. A twist distribution for near elliptic lift was identified as best concerning aerodynamic performance measured by the glide ratio or total drag at the design cruise condition.

2.3.2.2 Transonic Regime

Aerodynamics are especially challenging in conceptual design for the transonic regime. As with many aspects for unconventional aircraft, analytical methods inaccurately describe the physical effects of shock and wave drag effects. The Lock formula described and adapted by [6] for the estimation of wave drag effects is sufficient for preliminary estimates [7]. For validation, a comparison was performed with already available aerodynamic computations conducted within AIRBUS.

2.3.2.3 Stability and Control

The flight control surfaces of the ACFA BWB at this stage are ailerons, elevators, winglet rudders, slats, and flaps, in addition to spoilers and airbrakes. Unlike the CWB, no horizontal tail for trim can be used to trim the BWB. Instead, sweeping the wing and twisting the outer wing section is necessary. The influencing factors for flight control analysis in the preliminary design phase are weight in terms of MTOW and total wing span. Stability was analyzed with software, combining lifting line with vortex lattice and a 3D panel method. Additional analyses were conducted with calculations and available test data [14] based on [13].

2.3.3 Engine

The generic and scalable engine model used was provided by AIRBUS. It comprises a 115 klb take-off thrust engine and its characteristics during take-off, climb and cruise in regard to available thrust and fuel consumption. The model provided data for all relevant flight altitudes and temperature offsets from the International Standard Atmosphere (ISA), see Fig. 2.1.

Since two pylon-mounted engines are located over the center body of each configuration, scaling rules for the adaption of weight, specific fuel consumption (SFC), and dimensions were also implemented in agreement with AIRBUS. The take-off and initial climb is the decisive regime for the sizing of the engines and highly depend on the aerodynamic efficiency during acceleration and rotation. As in the conceptual development stage, the assessment of low-speed aerodynamics and take-off speeds is preliminary; a fixed thrust/weight ratio (T/W ratio) of 0.27 for both BWB and CWB was assumed. The engine size was computed according to (2.2):
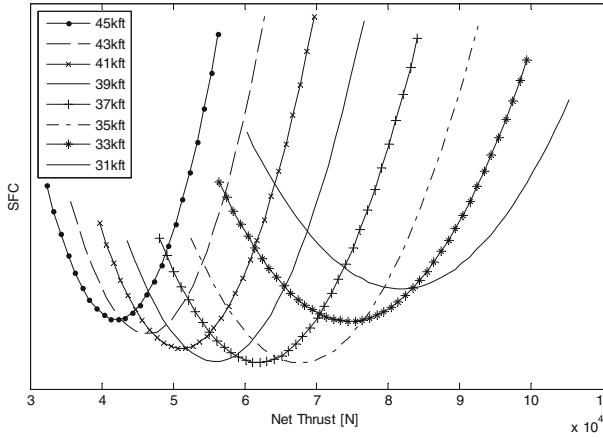
Fig. 2.1 Cruise specific fuel consumption (SFC) curves for BWB at different altitudes

$$F_{\text{engine}} \text{ (lbf)} = 0.27 \times \text{MTOW (kg)} \times 9.81 \text{ (m/s}^2)/(4.448222 \text{ (lbf/N)} \times n_{\text{engines}}[-]) \tag{2.2}$$

2.4 Multidisciplinary Design Optimization in the Structural Design Process

Details of the structural design of both ACFA 2020 aircraft concepts are given in the corresponding reports [9, 15]. Both concepts considered in the ACFA project are unconventional in nature, particularly with respect to the fuselage designs. Therefore, the applicability of traditional statistics-based mass estimation routines must be examined critically. In the case of the BWB configuration, the ACFA project was able to build upon experience from previous European framework programs, such as Very Efficient Large Aircraft (VELA) and New Aircraft Concepts Research (NACRE). For the CWB configuration, however, few data points were available. The design and mass estimate of the CWB fuselage was therefore performed in a closely coupled MDO process iterating between conceptual and structural designs.

Given the width of the cabin, a conventional circular cross-section pressure vessel is intangible for the CWB fuselage design, as this would lead to too much wasted space. Initial studies including, for example, elliptical cross sections quickly led to a so-called double-bubble design as a good trade-off between cross-sectional area and resistance to internal pressure loads. This design consists of two side-by-side pressure vessels supported by frames with a double-spherical section pressure bulkhead at the rear of the cabin. In the center, vertical struts connect the frames at the top and bottom surfaces and the floor beam. To determine the cross-sectional shape, an FE half-model of a section through the fuselage consisting of two frames, the outer skin, floor, and central supports was created and used as a basis of a multi-objective

Fig. 2.2 Design of the cross section: *Circled points* indicate design points of the spline; *boxes* are the prescribed dimensions for cabin and freight volume
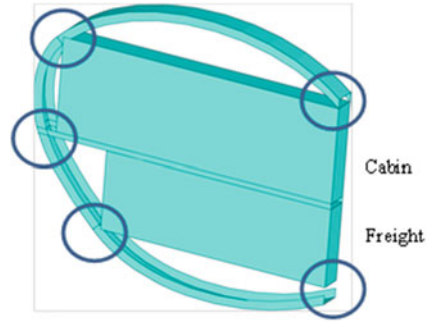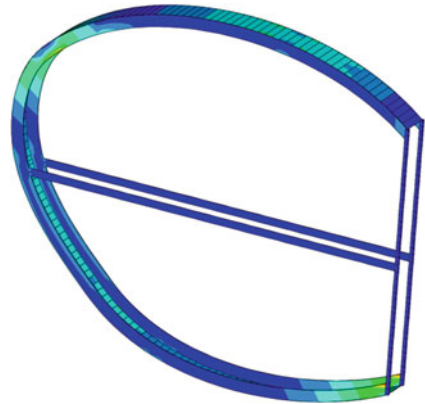

Fig. 2.3 Major principal strain in the fuselage cross section due to an internal pressure of 1 bar. Maximum strain (*green/yellow*) of 4.6‰


optimization of the structure (see Figs. 2.2 and 2.3). The shape of the cross section is given by four splines with support points at the corners of the boxes defining the payload volume provided by AIRBUS. The optimizer varies the distance of each control point from the payload circled in Fig. 2.2 and the slope of the spline, as well as the height of the frames at each point. An internal pressure of 1 bar is applied to the skin and symmetrical boundary conditions applied at the center line. The thickness of the skin and frames was kept constant. In addition to geometric constraints, the major principal strain in the structure was not allowed to exceed 5‰. The material was quasi-isotropic carbon fiber. The objective of the optimization was the minimization of a weighted sum of the normalized mass and the total cross-sectional and wetted area of the section.

After running the optimization with varying weighting of the two objectives, the resulting shapes and sectional masses were discussed with the conceptual design team. This resulted in the selection of the cross section shown in Fig. 2.3, with the mass of the section serving as the basis for the fuselage mass estimate.

In the case of the CWB wing box, the outer geometry was determined during the conceptual design stage, as well as the positions of front and rear spars. Position and length of a center spar were free to change during the structural design. The CWB

Fig. 2.4 Parameterized
model of the internal structure
of the CWB wing box with
variable rib spacing and
angle, as well as center spar
position and length
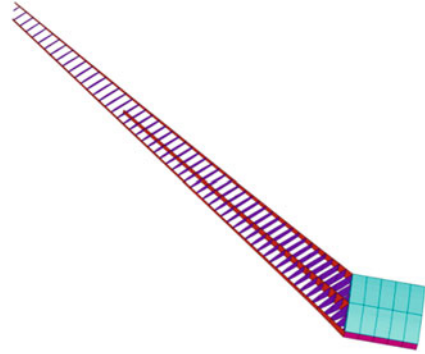
wing is thin and highly swept, but is generally of a conventional configuration and
thus expected to correspond well with statistical mass estimations.

To obtain a good configuration for the positioning of the wing box ribs, a para-
meterized FE model of the wing box was created as shown in Fig. 2.4, where the
outer skin has been removed in the figure to expose the ribs and center spar. In this
model, the position and length of the front and rear spars are constant, along with the
wing profile, twist, and dihedral. Spacing of the ribs in the wing box can be varied,
as can the angle between the ribs and the front spar. The chordwise position of the
center spar and its sweep and length can also be varied in the model. The model
has symmetric boundary conditions on the center plane. Elliptical pressure loads
simulating lift of a 2.5 g pull-up maneuver and of a -1.0 g push-over maneuver are
applied in two separate load cases with the weight of the fuselage included as dis-
tributed forces on the center part of the wing box in each case. Spar webs and ribs are
constructed of quasi-isotropic carbon-fiber-reinforced polymer (CFRP), wing skin,
and spar caps are highly orthotropic to take advantage of the well-defined load paths.
Stringers in the outer skin are modeled using layered shell elements; the top layer
modeled corresponding to the wing skin itself and subsequent layers are modeled
to the stringer webs and caps. These subsequent layers, therefore, have near-zero
stiffness orthogonal to the stringers, as well as a near-zero shear stiffness.

A parameter study of the internal structure of the wing box was performed using
a genetic algorithm [3]. Apart from the geometric variables described above, the
thickness of the wing skin and spar webs was also varied by the algorithm. In the
model, constraints are placed on the displacement at the tip and the major and minor
principal strains in the structure. However, since the primary failure mode of the wing
skin is expected to be skin buckling, a separate model was used to assess the stability
of the skin as shown in Fig. 2.5. During each evaluation, a skin panel between two
ribs near the wing root is automatically exported, re-meshed with a finer element
size, and the section forces from the global model are applied for each of the two
load cases. Finally, a linear buckling analysis is performed and the resulting load
factor is returned to the genetic algorithm.

Fig. 2.5 Buckling field between two ribs in the wing box
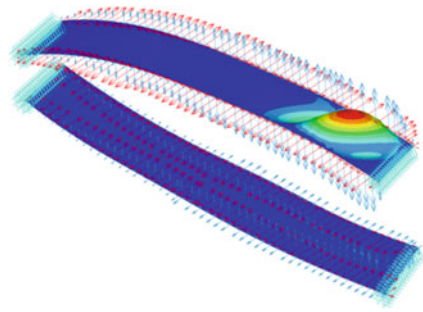
The objective function of the genetic algorithm was the mass of the wing box. After about 15 generations with a population size of 60, the algorithm had converged to a solution with a rib spacing of about 800 mm and an angle between ribs and front spar of about 95°. Buckling strength in both load cases was the limiting constraint.

With the finalized topology of the wing box structure, a structural sizing optimization of the FE half-model, including the fuselage, tail and simplified engine mountings, was performed. Mass modeling was performed in cooperation with the conceptual design, distributing nonstructural masses representing landing gears, and other equipment in the fuselage according to the conceptual mass estimate. Likewise, a mass point representing the engine is positioned at the center of gravity of the engine and connected by rigid beams to the fuselage. Fuel masses are distributed in the wing and connected via rigid-body elements to the wing box. Symmetric boundary conditions are applied at the center plane. An elliptical pressure distribution representing the lift in both the positive 2.5 g maneuver as well as the −1.0 g maneuver was applied to the wing (see Fig. 2.6), a constant pressure was applied to the tail surfaces (see Fig. 2.7), and an internal pressure of 1.4 bar was applied to the fuselage between the pressure bulkheads at the rear and the nose.

In order to further improve the model, stringers in the wing skin were modeled as beam elements with the skin as a single-layer orthotropic shell. Stringers in the fuselage, tail and stabilizers were modeled in the same manner.

The sizing optimization of the half-model comprised 54 design variables consisting of the thickness of the wing skin separated into several design zones, the thickness of the fuselage skin similarly divided into zones and thickness of the stabilizer skin,

Fig. 2.6 Elliptical lift distribution applied to the wing distribution for structural sizing
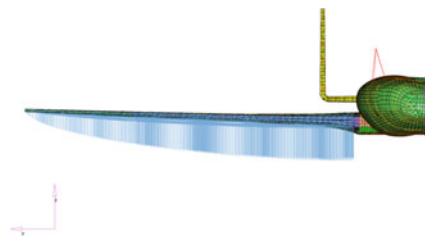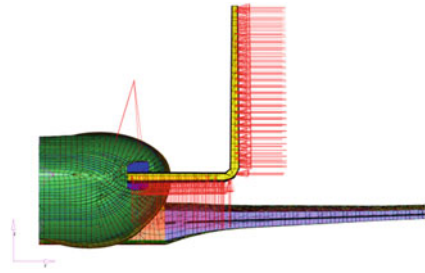
shear webs of the fuselage frames, as well as spars and ribs in the wing and stabilizer. Dimensions of the stringers in the wing, stabilizers, and pressure hull were also variable, as well as the dimensions of the caps of spars and ribs in the wing and stabilizer, in addition to the caps of the frames in the fuselage. Elastic strain in the structure was constrained to remain within $\pm 5\%o$. The objective of the optimization was minimum structural mass.

Convergence was generally rapid with a candidate optimal solution usually delivered in less than 35 iterations with stringent convergence criteria. Starting the optimization from several starting points resulted in the selection of an optimum design on which to base the final structural design.

The design resulting from the sizing optimization is intuitive: strength-limited components (that is, those close to the strain limit) are the wing skin near the wing root, the fuselage skin where the wing box passes through the hull and the stringers in the wing to around 2/3 of the span. Also following intuition, the thickness of the wing skin decreases when going from root to tip and thicknesses of shear webs in spars and frames tend to their minimum values, since no constraints on the stability of these components were included. Sizing variables of the stabilizers all tend to their minimum values indicating that the loads applied to them might need to be reviewed.

Comparing the mass of the final structural design with the initial mass estimates of the conceptual design results in a difference of about 5 % for the wing with the structural model mass being greater. This rather small difference is consistent with the conventional design of the wing. In the fuselage, the structural model mass is almost 15 % lighter than the conceptual design, despite the latter being based on the original FE section model. Similarly, the mass of the stabilizers in the structural model is 20 % less than the initial estimate. The most likely explanation for these discrepancies is lack of dimensioning load cases, such as impact at landing or the loss of an engine at take-off, as well as nonconservative sizing rules for the shear webs and skins in the hull considering only static strength and not stability.

Finally, a more detailed aeroelastic tailoring was performed of the wing box in isolation [11]. Mass and inertia properties of the rest of the structure were concentrated at a mass point located at the center of gravity and this was connected to the wing box using rigid elements as shown in Fig. 2.8. Modeling of the tail was greatly simplified. It was connected to the mass point at the center of gravity using beam elements whose mechanical properties were determined from the detailed FE

Fig. 2.8 FE model of wing
with simplified tail surfaces
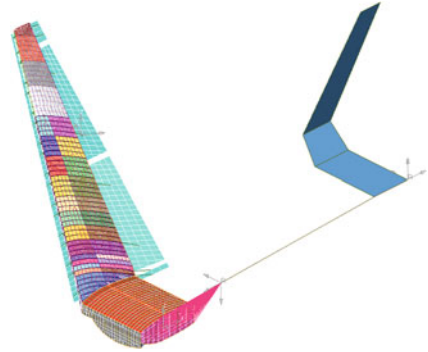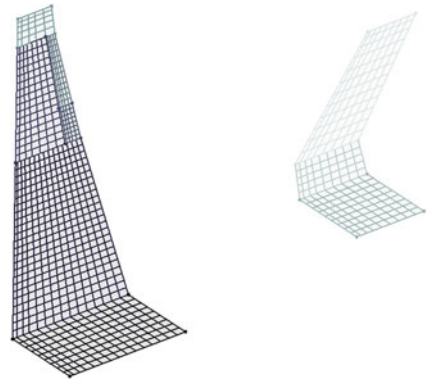for aeroelastic tailoring

Fig. 2.9 DLM mesh of wing
and tail including split aileron
vertical stabilizer and trim
surface

model of the fuselage. Flaps and slats were included as plates with approximated mass and stiffness properties and fastened to the wing box without stiffening it in bending. Boundary conditions were applied at the center of gravity; both symmetric and anti-symmetric cases were included.

In addition to the structural model, a DLM was created as shown in Fig. 2.9. The aerodynamic model includes the wing and tail surfaces, as well as the split aileron.

The 2.5 and -1.0 g static load cases were simulated by trimming the aircraft with the corresponding constant vertical acceleration using the horizontal tail surface (excluding the part of the tail contained within the fuselage). In addition, positive and negative roll maneuvers due to deflection of each of the ailerons or both of them together were included. The response to discrete $1 - \cos$ gusts of various lengths was also assessed.

For aeroelastic tailoring, the wing skins were modeled as four-layer shells with one layer for each fiber orientation, $0°$, $90°$, and $\pm45°$ with properties smeared across the thickness of the shell. The optimizer was free to vary the thickness of each layer separately. Constraints, as before, were placed on the elastic strain in the material. Additionally, a constraint was placed on the minimum steady-state roll rate to ensure control effectiveness and on the difference between first bending and torsional

eigenfrequencies to avoid flutter problems. As previously, the objective was to minimize mass.

The tailored design does not differ significantly from the previous sizing of the wing box, except at the outer third of the span where additional stiffness, and therefore material, must be added to the wing to ensure compliance with the roll effectiveness constraint. The critical gust loads (both positive and negative) also lead to excessive strains in this region requiring reinforcement, whereas the strength at the wing root after sizing for the static maneuver cases is adequate. The main reason for the critical loads at this location is because the center spar ends here which modifies the shear flow for torsional loads.

2.5 Configuration Selection

The one-year conceptual design process demonstrated the feasibility of both aircraft concepts. Selected results will be presented in this section leading to a comparison and thus selection of the BWB concept over the CWB design.

2.5.1 Results

Selecting a future aircraft layout within the ACFA framework was conducted based on a detailed trade-off analysis comprising the categories geometry, aerodynamics, weights, and mission performance. The work in this section represents first year-end collaborative research results [8, 12]. Figure 2.10 depicts the two basis configurations with their main dimensions.

2.5.1.1 Geometry

The CWB in its final configuration has a wing aspect ratio of 10.83, whereas the BWB has a ratio of only 4.82 due to its unconventional form. One reason is the 80 m wing span limitation. The all-lifting BWB airframe results in a low required C_L in cruise and low induced drag.

The increased lifting surface and reference area of the BWB potentially increases low-speed lift. The detailed trade-off for cruise drawbacks for flying in higher altitudes can be significant. Although the reference area of the BWB is much larger, the overall wetted area is 3.6 % less leading to lower zero lift friction drag. Taper ratios are 0.09 for the BWB and 0.29 for the CWB.

The CWB fuselage accommodating the passenger cabin is 14.77 m longer. The reason for this is the widening of the cabin box along the y-axis in the BWB. Effects on ride comfort were evaluated later in the project. The current CWB and BWB configuration can house at least 30 LD3 containers. Both concepts position the
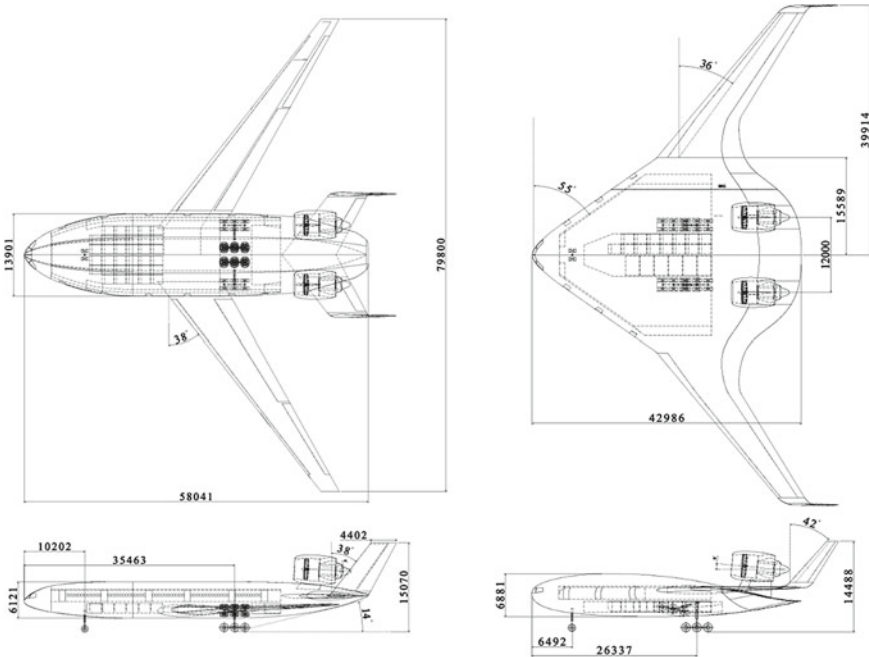
Fig. 2.10 Overview of CWB (*left*) and BWB (*right*)

engines on top of the fuselage with possible shielding effects expected to be larger for the BWB. However, no significant structural advantages are expected, since the structural reinforcements of conventional under-wing engine mounting are also required for the envisaged central aft mounting.

For yaw control, the CWB configuration uses double fins with rudders, whereas the BWB uses winglets with a rudder chord of 30 % of the winglet.

Trim is also challenging. Neglecting trim drag on the BWB seems a reasonable approach as it can be assumed that fuel transfer between the different central and outboard fuel tanks could be used to have the aircraft center of gravity (CG) aligned with the center of pressure in cruise without having to deflect the elevators, so without creating trim drag. This is a target approach assuming that it is possible to design the fuel system in such way that it could cope with the CG variation due to different payload level (baggage and passengers) and variation of fuel volume on-board along the flight. The approach seems reasonable given the significant internal volume in the wing and in the center body of the BWB that gives enough flexibility to install the fuel tanks appropriately. A study on the ACFA 2020 BWB configuration has been done in [16]. The same kind of approach has been used within Airbus for internal projects on BWB in the recent years.

All trailing edge movables are needed on the BWB. In comparison, the CWB has a heavy movable H-tail, which counteracts center of gravity shifts during flight

more easily and with fewer flight dynamics interactions. Damping capabilities for flight stability are generally lower on the BWB due to smaller lever arms and higher coupling effects. However, more sophisticated approaches are necessary to perform a detailed stability and performance assessment.

2.5.1.2 Aerodynamic Performance and Stability

The BWB has a better lift/drag ratio (L/D ratio) at the reference Reynolds number and a very low C_{D0}, since the ratio of wetted area to S_{ref} is lower. As the BWB aspect ratio is also low, induced drag increases rapidly with C_L and leads to very low optimum C_L of 0.25 for the BWB. Opposite effects lead to a higher optimum C_L of 0.47 on the CWB [12]. Hence for the total lift force in cruise, the lower C_L for the BWB requires a larger wing area. Figures 2.11 and 2.12 depict the lift distribution along the span for CWB and BWB. CWB distribution is close to an elliptic lift distribution which results in low induced drag. Figure 2.12 shows the lift distribution of the BWB at the due date of the configuration selection and indicates the need for further modification of the lifting body geometry. The final configuration and lift distribution is presented in [7].

Stability analysis revealed a slightly stable (1 % static margin) configuration and the need for more detailed models since the margin range is small and the accurate determination in preliminary design with conventional methods is challenging.

2.5.1.3 Weights

Comprehensive data for all system and structure weights was computed. Especially for highly complex elements of the overall aircraft, the methods from conventional
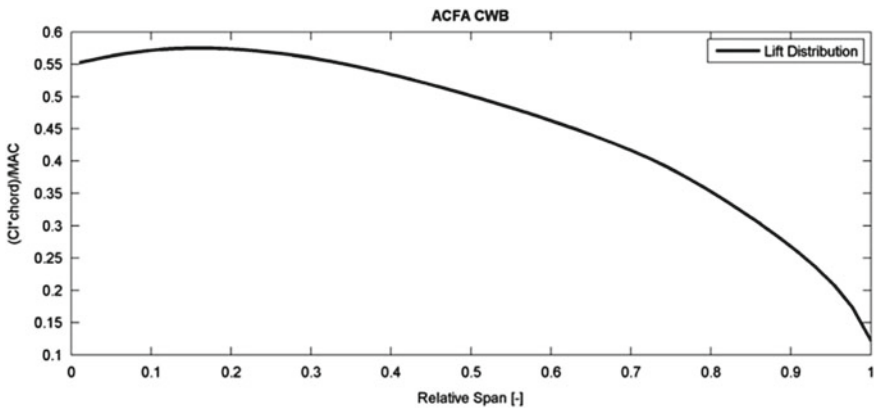

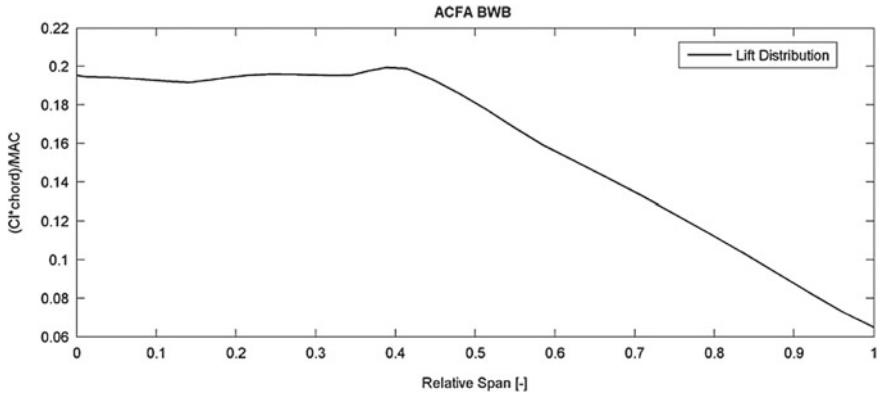**Fig. 2.11** ACFA CWB lift distribution

Fig. 2.12 ACFA BWB lift distribution

aircraft design need refinement. The BWB aircraft realizes a weight advantage of 14.10 t. The horizontal and vertical stabilizers on the CWB add a 25.6 % weight penalty, since conventional tail horizontal stabilizers on the BWB do not exist. Because operator items are assumed to be equal for both configurations, the BWB achieves an OWE advantage of 9.7 t over the CWB. Both configurations are separated by a 23.79 t MTOW advantage for the BWB.

2.5.1.4 Engine

Based on the calculations in preliminary design and the CWB's lower optimum altitude, CWB thrust per engine is 126.7 klb sized for the minimum T/W ratio of 0.27. BWB cruise and stepped altitude requirements lead to thrust of 119.6 klb per engine.

2.5.2 Aircraft Selection

As the conceptual aircraft design has revealed, both configurations offer promising advantages for future air transport (see Table 2.2). The BWB's weight benefit is significant and the inferior cruise and resulting fuel burn performance of the CWB, whose cruise L/D is 21.7 compared to 24.2 of the BWB, is a further disadvantage of the CWB. The higher flight altitudes for the BWB and thus the required engine thrust does not exceed what current engines available on the market can deliver.

For its superior mission performance in fuel consumption on a 7,200 nm (4,000 nm) mission, the BWB beats the CWB by more than 13 %. No development obstacles have been identified; hence the BWB was studied and optimized in the detailed development phase of the ACFA 2020 project.

Table 2.2 Mission performance comparison for BWB and CWB [12]

	BWB	CWB	Δ (%)
TOW	401.6 t	428.4 t	−6.7
OWE	255.0 t	234.7 t	8.0
2-Class Pax capacity	470	464	1.3
Engine size	119.6 klb	126.7 klb	−5.9
CL of L/Dmax	0.25	0.47	
L/Dmax	24.2	21.7	10.3
Block fuel 4,000 nm	62.03 t	68.16 t	
	131.8 kg/Pax	146.9 kg/Pax	−11.5
Block fuel 7,200 nm	116.47 t	130.25 t	
	247.8 kg/Pax	280.7 kg/Pax	−13.3
Initial cruising altitude (ICAC)	36,000 ft	33,100 ft	8
TTC at 31,000 ft	25.6 min	25.6 min	0

2.5.3 Conclusion and Outlook

Within the project time frame of one year, two conceptual commercial aircraft designs for a long-haul mission were developed and compared based on a comprehensive set of requirements. The selection process was driven by the mission performance calculations based on geometric, aerodynamic, and weight analysis. Furthermore, a comprehensive MDO was performed to optimize fuselage cross section and wing box design.

The selection of the BWB is a result of its superior efficiency. Compared to an improved wide body design such as the CWB, the mission performance results in 15.46 t less fuel burn with corresponding CO_2 savings.

Ongoing research in the field of aircraft design addresses the preliminary design process adoptions and the design for active control technologies [7]. Especially in the areas of stability analysis, transonic aerodynamics and structure, conventional methods need adjustments in order to efficiently apply them in conceptual design. Ride comfort and passenger acceptance, as well as the inclusion of these radical configurations in the controlled airspace, are issues necessitating further research.

Additional improvements to reach the ACARE goals and to lower fuel consumptions beyond what can be achieved by new airframe designs are expected from innovative engine technologies and more efficient air traffic management.

References

1. Hileman J, Spakovszky Z, Drela M, Sargeant M (2007) Airframe design for "Silent Aircraft". In: 45th AIAA aerospace sciences meeting and exhibit, Reno, Nevada, USA
2. IABGmbH. Luftfahrttechnisches Handbuch (LTH) (2008) (English: Aviation Technology Handbook). Ottobrunn, Germany. http://www.lth-online.de. Accessed 8 July 2014
3. Langer H (2005) Extended evolutionary algorithms for multiobjective and discrete design optimization of structures. PhD thesis, Technische Universität München, Munich, Germany
4. Leahy J (2010) Airbus global market forecast 2010–2029. Toulouse, France
5. Liebeck RH (2004) Design of the blended wing body subsonic transport. J Aircr 41(1):10–25
6. Malone B, Mason WH (1995) Multidisciplinary optimization in aircraft design using analytic technology models. J Aircr 32(2):431–438
7. Mohr B, Paulus D, Baier H, Hornung M (2012) Design of a 450 passenger blended wing body aircraft for active control investigations. J Aerosp Eng 226(12):1513–1522
8. Mohr B, Plötner K, Rößler C (2010) ACFA 2020 WP 1. Final report. Munich, Germany
9. Paluch B, Joly D (2010) D1.2 Part 1: design steps of the BWB finite element model. Lille: ONERA, France
10. Paulus D, Salmon T, Mohr B, Rößler C, Petersson Ö, Stroscher F, Baier H, Hornung M (2013) Configuration selection for a 450-passenger ultraefficient 2020 aircraft. Prog Flight Dyn GNC Avionics 6:601–618
11. Petersson Ö, Stroscher F, Baier H (2010) Multidisciplinary optimisation of aircraft wings including gust loads. In: 2nd aircraft structural design conference, London. Royal Aeronautical Society
12. Salmon T (2009) Comparison dossier of the two 450 passenger aircraft configurations for ACFA 2020, ACFA 2020 D1.5. Chatillon, France
13. Schemensky RT (1973) Development of an empirically based computer program to predict the aerodynamic characteristics of aircraft. Technical report, Air Force Flight Dynamics Laboratory. AFFDL-TR-73-144
14. Staudacher W (2011) ACFA BWB conceptual design calculations. Munich, Germany
15. Stroscher F, Petersson Ö, Baier H (2009) D1.3 Part 2: structural design of the ACFA 2020 CWB configuration, Munich, Germany
16. Wildschek A, Stroscher F, Haniš T, Belschner T (2013) Fuel management system for cruise performance optimization on a large blended wing body airliner. In: Progress in flight dynamics, guidance, navigation, control, fault detection, and avionics, vol 6. EDP Sciences, pp 651–670